Development of a High Fundamental Frequency (HFF) Piezoelectric Immunosensor for Early and Sensitive Detection of Tuberculosis

Angel Montoya [*a], Carmen March[a], Yeison J. Montagut[b], María J. Moreno[a], Juan J. Manclús[a], Antonio Arnau[a,c], Yolanda Jiménez[a,c], Marisol Jaramillo[b,d], Paula A. Marín[b] and Róbinson A. Torres[b]

[a]*Centro de Investigación e Innovación en Bioingeniería (Ci2B), Universitat Politècnica de València. Valencia, Spain;* [b]*Escuela de Ingeniería de Antioquia (EIA) - Universidad CES, Medellín, Colombia;* [c]*Advanced Wave Sensors (AWS), Valencia, Spain;* [d]*Universidad Nacional de Colombia*

Abstract: Tuberculosis, one of the oldest diseases affecting human beings, is still considered as a world public health problem by the World Health Organization. Therefore, there is a need for new and more powerful analytical methods for early illness diagnosis. With this idea in mind, the development of a High Fundamental Frequency (HFF) piezoelectric immunosensor for the sensitive detection of tuberculosis was undertaken. A 38 kDa protein secreted by *Mycobacterium tuberculosis* was first selected as the target biomarker. Then, specific monoclonal antibodies (MAbs) were obtained. Myc-31 MAb, which showed the highest affinity to the analyte, was employed to set up a reference enzyme-linked immunosorbent assay (ELISA) with a limit of detection of 14 ng mL^{-1} of 38 kDa antigen.

For the development of the HFF piezoelectric immunosensor, 100 MHz quartz crystals were used as transducer elements. The gold electrode surface was functionalized by covalent immobilization of the target biomarker through mixed self-assembled monolayers (mSAM) of carboxylic alkane thiols. A competitive immunoassay based on Myc-31 MAb was integrated with the transducer as sensing bio-recognition event. Reliable assay signals were obtained using low concentrations of antigen for functionalization and MAb for the competitive immunoassay. Under optimized conditions, the HFF immunosensor calibration curve for 38 kDa determination showed a limit of detection as low as 11 ng mL^{-1} of the biomarker. The high detectability attained by this immunosensor, in the picomolar range, makes it a promising tool for the easy, direct and sensitive detection of the tuberculosis biomarker in biological fluids such as sputum.

Keywords: Tuberculosis; 38 kDa Biomarker; Monoclonal Antibody; ELISA; High Fundamental Frequency (HFF); Piezoelectric Immunosensor

1. INTRODUCTION

Tuberculosis (TB) is a public health problem that affects millions of people around the world, and it is the second cause of death due to infectious illness after the Human Immunodeficiency Virus. According to reports by the World Health Organization, more than nine million new cases of TB are reported every year, resulting in the deaths of approximately two million people. Currently, one of the main challenges in controlling TB is the implementation of alternative diagnosis methods for early detection [1],[2].

Many tests developed for TB diagnosis are based on molecular biology techniques, which give results in a few hours. However, their routine use in vulnerable endemic areas is reduced by the costs of this technology and the high level of technical training needed for health professionals. Therefore, in many affected areas the strategy for controlling the illness is still based on the sputum coloration and culture. The main disadvantage of these traditional methods is the long time required before results are available, which affects the opportune starting of treatment, thereby increasing the rates of the illness spreading [3].

*Address correspondence to Angel Montoya at Centro de Investigación e Innovación en Bioingeniería (Ci2B), Universitat Politècnica de València, Camino de Vera, s/n, 46022 Valencia, Spain; Tel/Fax: +34 963877093; E-mail: amontoya@eln.upv.es

As a response to these limitations in current detection techniques, alternative detection methods based on biosensors have been developed [4]-[10]. As known, biosensors are analytical devices that integrate a biological component (the bio-receptor) with an electronic or optoelectronic transducer to detect and quantify the presence of target analytes in complex samples. In a very recent report [11], the state of the art and the main analytical performance, advantages and drawbacks of different biosensor approaches to the detection of tuberculosis are exhaustively reviewed. To date, electrochemical, optical, mechanical (including piezoelectric) and magnetic biosensors have been or are being developed, with different sensitivities. The reported limits of detection are highly variable among devices, ranging from 20 to 10^7 colony forming units (CFU) per mL for *Mycobacterium tuberculosis* (*Mbt*) cells or from 0.1 to 30 ng mL^{-1} for different biomarker antigens.

Biosensors using immunoreactive bio-receptors and piezoelectric crystals working in the Quartz Crystal Microbalances (QCM) mode as transducers are known as piezoelectric immunosensors [12]. A piezoelectric crystal acting as a QCM allows the measurement of changes in the surface mass density that occur in an infinitesimally thin layer in contact with the crystal, considered to be rigid. Changes in this thin layer modify the piezoelectric

electroacoustic properties of the sensor. Two methods are used in biosensors to obtain mass variation, based on the measurement of one of the sensor electric variables: resonance frequency and phase.

The first method is based on the continuous measurement of the crystal resonance frequency (***f***). The resonance frequency variation is related to variations in the surface mass density deposited on the crystal surface according to Sauerbrey's equation [13]:

$$\Delta f = -(2f_0^2/Zcq)\rho_s = -C_{SB}\,\rho_s \qquad \text{(Eq. 1)}$$

Where:

f_0: Resonance frequency in vacuum.
Zcq: Acoustic impedance characteristic of quartz.
ρ_s: Surface mass density (density of the thin layer deposited on the crystal).
C_{SB}: Sauerbrey's coefficient.

The second method is based on interrogating the piezoelectric crystal with a signal at a constant frequency near the crystal resonance frequency and measuring the signal phase (***φ***). The changes produced in the signal phase are related to the mass variations on the crystal surface according to the phase equation [14]:

$$\Delta\varphi = -(\Delta m_S/m_L) \qquad \text{(Eq. 2)}$$

Where:

m_s: Surface mass density in contact with the crystal
m_L: Effect of the liquid displaced by the crystal

An infinitesimally thin rigid layer can be generated on the surface of a quartz crystal gold electrode by covalent immobilizing through a self-assembled monolayer (SAM) of an immunoreagent (an antigen or an antibody). When the functionalized piezoelectric sensor is put in contact with a complex sample, the antigen-antibody interactions that occur between the immunoreagent immobilized on the crystal and those in the sample modify the electric properties of the QCM. This allows to establish a clear relationship between the variations of analyte concentration in the sample and mass-related signal changes in the sensor.

Piezoelectric biosensors have been reported for detection or diagnosis of diseases such as hepatitis C [15], hepatitis B [16], thalassemia [17], malaria [18] and human papilloma virus [19]. Although QCM offer many benefits, including low cost, ease of use, real-time analysis and direct detection capability without the need of labelling, the development of piezoelectric biosensors applied to the diagnosis has been seriously affected by the low sensitivity offered by the usual low-frequency (below 50 MHz) QCM devices. Recently, advances in piezoelectric technology led to the development of high fundamental frequency microbalances (HFF-QCM) that allow for two orders of magnitude increased sensitivity [20], which could be useful for the detection of tuberculosis biomarkers. This way, HFF-QCM devices could provide effective, fast and accessible alternative methods for TB detection, meeting analytical performance requirements such as high sensitivity, rapidity in providing results, ease of use and even portability [21].

Some piezoelectric immunosensors have been reported to be able to detect TB [22],[23]. These biosensors are based on low-frequency QCM sensors and on direct immunoassays with immobilized antibodies for the detection of *Mbt* CFUs or biomarkers. With this frequency and assay configuration, the biosensor sensitivity and the biochemical stability of the antibodies were too poor, which seriously affects the usefulness of the biological interface and increases the cost of immobilization.

In the present paper, the development of an HFF-QCM piezoelectric immunosensor for highly sensitive detection of a TB biomarker is described. To this purpose, the 38 kDa antigen from *Mbt* was first selected as the disease biomarker. This lipo-glyco-protein is one of the immunodominant antigens in the microorganism and is considered as a good indicator of both the progress of the illness and the effectiveness of the treatment [24],[25]. Consequently, the 38 kDa antigen is among the most widely used biomarkers in the development of TB diagnostic methods based on immunoassays [26]-[28].

Monoclonal antibodies (Mab) specific to the target biomarker were obtained. The highest-affinity one was used as the primary immunoreagent for the development of a competitive enzyme-linked immunosorbent assay (ELISA) for 38 kDa quantification. This ELISA was used as a previous diagnostic test and reference assay for the biosensor. Finally, the HFF piezoelectric immunosensor was developed for the detection and quantification of the 38 kDa antigen. High frequency (100 MHz) quartz crystals were used as biosensor transducers. The crystals were functionalized by covalently immobilization of the 38 kDa antigen on the surface of the quartz crystal gold electrode and a monoclonal antibody-based competitive immunoassay was integrated as the sensing specific bio-recognition event coupled to the transducer. The analytical performance of the developed ELISA and HFF-QCM immunosensor are presented and discussed.

2. MATERIALS AND METHODS

2.1. Reagents and instruments

2.1.1. General:

Bovine serum albumin (BSA) fraction V was purchased from Roche Diagnostics (Mannheim, Germany). Tween-20 was from by Fluka-Aldrich Chemie (Buchs, Switzerland). All other chemicals were of analytical grade. Flat bottom polystyrene ELISA plates (High Binding Plates) were from Costar (Cambridge, MA). 100 MHz HFF-QCM crystals were from AWSensors (Valencia, Spain).

2.1.2. Immunoreagents:

The selected antigen for mouse immunization was a recombinant form of the 38 kDa protein from *Mbt*. It was supplied by MyBioSource (San Diego, CA). The same antigen was also used for ELISA plate coating and for covalent immobilization onto piezoelectric crystals. Peroxidase-labeled rabbit anti-mouse immunoglobulins were obtained from Dako (Glostrup, Denmark).

2.1.3. Reagents for covalent immobilization:

1-ethyl-3 (-3 dimethyl-amino-propyl) carbodiimide hydrochloride (EDC) and N-hydroxysuccinimide (NHS) were purchased from Pierce (Rockford, IL); mercaptohexadecanoic acid (MHDA) and 11-mercaptoundecanol (MUD) were supplied by Sigma-Aldrich

Chemie (Steinheim, Germany); ethanolamine blocking agent was obtained from Sigma (St. Louis, MO).

2.1.4. Apparatus

ELISA plates were washed with a 96PW microplate washer from SLT Labinstruments GmbH (Salzburg, Austria). Absorbance was read in dual-wavelength mode (490–650 nm) with an Emax microplate reader from Molecular Devices (Sunnyvale, CA). All Immunosensor assays were performed in the AWS A20 test platform combined with the F20 flow module recently developed by AWSensors (www.awsensors.com).

2.2. Monoclonal antibody production.

The usual steps involved in hybridoma technology were followed:

2.2.1. Mice immunization:

Five female BALB/c mice (8-10 weeks old) were immunized with the recombinant 38 kDa biomarker from *Mycobacterium tuberculosis*. First dose consisted of 50 µg of the antigen intraperitoneally injected as an emulsion of PBS (10 mM phosphate buffer, 137 mM NaCl, 2.7 mM KCl, pH 7.4) and complete Freund's adjuvant. Two and four weeks after the initial dose, mice received booster injections with the same amount of antigen emulsified in incomplete Freund's adjuvant. One week after the last injection, mice were tail-bled and sera were tested by ELISA for the presence antibodies recognizing the 38 kDa antigen. After a resting period of at least three weeks from the last injection in adjuvant, mice received a final soluble intraperitoneal injection of 50 µg of antigen in PBS, four days prior to spleen extraction and cell fusion.

2.2.2. Cell fusion:

P3-X63/Ag 8.653 murine myeloma cells (ATCC, Rockville, MD) were cultured in high-glucose Dulbecco's Modified Eagle's Medium supplemented with 2 mM glutamine, 1 mM nonessential amino acids, 25 µg/ml gentamicin, and 15% fetal bovine serum (referred to as s-DMEM, GIBCO, Paisley, UK). Cell fusions were carried out essentially as previously described [29]. In summary, mouse spleen lymphocytes were fused with myeloma cells at a 5:1 ratio using Polyethylene Glycol 1500 (Roche Applied Science, Mannheim, Germany) as the fusing agent. The fused cells were distributed in 96-well culture plates at an approximate density of 2 x 10^5 cells/100 µl of s-DMEM per well. Twenty-four h after plating, 100 µl of HAT selection medium (s-DMEM supplemented with 100 µM hypoxathine, 0.4 µM aminopterine, 16 µM thymidine) containing 2% Hybridoma Fusion and Cloning Supplement (HFCS, Roche) was added to each well. Half the medium of the wells was replaced by fresh HAT medium on days 4 and 7 post-fusion. Cells were grown in HAT medium for 2 weeks and then HAT was substituted by HT medium (HAT medium without aminopterine).

2.2.3. Hybridoma Cloning:

Eight to ten days after cell fusion, culture supernatants were screened by ELISA for the presence of antibodies that recognized the 38 kDa target biomarker. Selected hybridomas were cloned by the limiting dilution method using HT medium. Stable antibody-producing clones were expanded and cryopreserved in liquid nitrogen.

2.2.4. Monoclonal antibody purification:

MAbs were purified from late stationary phase culture supernatants by saline precipitation with 50% saturated ammonium sulphate followed by affinity chromatography on protein G-Sepharose 4 Fast Flow (GE Healthcare Bio-Sciences, Uppsala, Sweden). Purified MAbs were finally stored at 4 °C as ammonium sulfate precipitates.

2.3. ELISA development.

ELISA plates were coated overnight with the recombinant 38 kDa antigen in 50 mM carbonate buffer, pH 9.6. A volume of 100 µL per well was used trough all immunoassay steps. All incubations were carried out at room temperature. After each incubation, plates were washed four times with washing solution (0.15 M NaCl containing 0.05% Tween 20).

2.3.1. Non-competitive ELISA:

A non-competitive indirect ELISA in the antigen-coated format was used to estimate mouse serum antibody titers, for the characterization of culture supernatants and antibodies, and for checkerboard titration to determine the optimal conditions for the quantitative competitive ELISA. Plates were coated with the 38 kDa antigen at appropriate concentrations. Then, 100 µL of serum, culture supernatant or antibody dilution in PBS was added and incubated for 1 h. Next, plates were incubated for 1 h with peroxidase-labeled rabbit anti-mouse immuno-globulins diluted 1/2000 in PBST (PBS containing 0.05% Tween 20). Finally, peroxidase activity bound to the wells was determined by adding the substrate solution (2 mg/mL OPD and 0.012% H_2O_2 in 25 mM citrate, 62 mM sodium phosphate, pH 5.35). After 10 min, the reaction was stopped with 2.5 M sulphuric acid, and the absorbance was read at 490 nm.

2.3.2. Competitive ELISA for 38 kDa quantification:

An indirect competitive ELISA was developed for the quantification of the target biomarker. The procedure was the same as for the non-competitive ELISA except that after coating a competition step was introduced by adding 50 µL/well of 38 kDa antigen standards, followed by 50 µL/well of the appropriate concentration of purified Myc-31 monoclonal antibody. Optimal concentrations of the 38 kDa antigen for coating (0.05 µg mL^{-1}) and MAb in solution for the competition step (0.05 µg mL^{-1}) were first determined by checkerboard titration.

2.4. HFF-QCM sensor set-up.

2.4.1. HFF-QCM sensor chip and flow cell assembly:

Sensors were from AWSensors (Valencia, Spain). They were based on square shaped 100 MHz AT-cut, inverted mesa crystals, with a total area of 36 mm^2 and an etched area thickness of around 17 µm. The electrode active surface was of 0.785 mm^2 for 1.00 mm electrode diameter. 100 MHz piezoelectric crystals were assembled on a polyether ether ketone (PEEK) support and HFF-QCM chips were subsequently mounted into a flow-cell suitable for operation at high frequencies as previously described [20].

2.4.2. Measurement platform:

The flow cell was included in the AWS A20 test platform, which was combined with the F20 flow module from AWSensors (Fig. 1). AWS A20 platform consists basically on an electronic characterization system based on the fixed frequency phase-shift measurement technique described elsewhere [14]. F20 module is a flow-through automated equipment controlled by syringe pumps (Hamilton, Bonaduz, GR, Switzerland). This way, samples were delivered to the flow cell at a constant flow rate. Both modules were kept at 25 ºC. Both AWS A20 platform and F20 flow module were controlled (data acquisition and analysis and fluidics) by AW-BIO v1.8 dedicated software (AWSensors, Spain). Phase, amplitude and temperature were measured, recorded and processed through the assays.

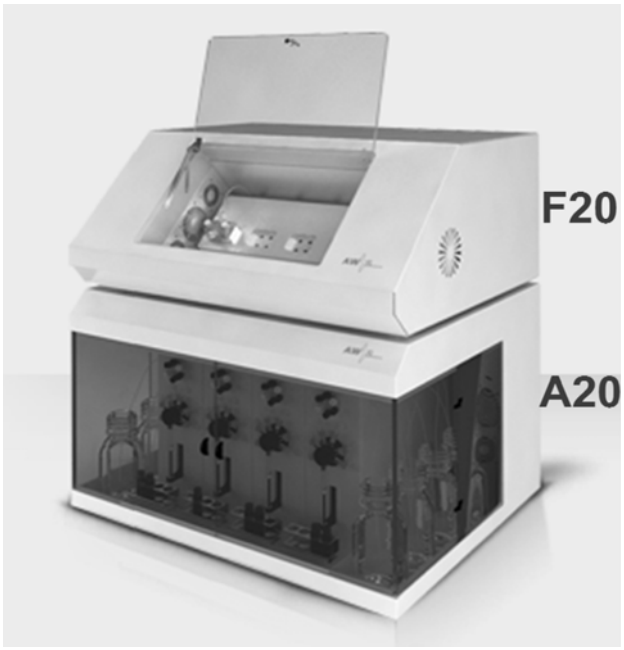

Figure 1. A20 test platform and F20 flow module developed by AWSensors and used in the present study.

2.5. Sensor functionalization.

Sensor functionalization was carried out by means of covalent immobilization of the recombinant 38 kDa antigen on the gold electrode surface of 100 MHz HFF-QCM crystals. Prior to immobilization, chips were subjected to UV-ozone radiation for 15-20 min using a UV/Ozone ProCleaner from BioForceNanosciences (Ames, IA). Crystals were then rinsed with distilled water and ethanol and blown dry by a nitrogen stream.

The covalent immobilization was carried out by means of classic amide chemistry. Mixed self-assembled monolayers (mSAM) of carboxylic alkane thiols were used as intermediate layers for immobilization. All procedures were performed on only one face of the crystal following the previously described protocol [30] except for the composition of the mSAM and the protein to be immobilized. The mSAM was composed by a 250 µM mixed solution of MHDA and MUD (1:20 molar ratio). The protein to be immobilized was the recombinant 38 kDa antigen. It was prepared at 10, 20 and 50 µg mL^{-1} in PBS and placed for 4 h on previously activated crystal surfaces.

2.6. Immunoassay format in the HFF immunosensor.

A binding inhibition test was develop and coupled to the functionalized sensors in order to determine the 38 kDa tuberculosis biomarker with the HFF-QCM. It consisted of a competitive immunoassay in the antigen-coated format. To this purpose, a fixed amount of the selected monoclonal antibody (Myc-31) was mixed with standard solutions of the 38 kDa antigen at different concentrations, and the mixtures were pumped over the sensor surface where the same protein had been previously immobilized. Since the free analyte (biomarker) inhibits the antibody binding to the same immobilized antigen, the assay signal of the piezoelectric sensor (phase shift) will decrease as the biomarker concentration increases.

Standard 38 kDa solutions rangin from 10^{-3} to 10^{2} µg L^{-1} were prepared by serial dilutions in PBS and mixed with an equal volume of a 0.75 µg mL^{-1} solution of Myc-31 MAb. Analyte-antibody mixtures were incubated for 1 h at room temperature and then 650 µL of this mixture were brought onto the functionalized sensor surface. Variations in phase response were monitored in real time as the binding between the free antibody and the immobilized recombinant 38 kDa protein took place. Regeneration of the functionalized surfaces to break the antigen-antibody association was accomplished with 0.05 M HCl.

Standards were run at least in duplicate. Calibration curves were obtained by plotting the phase decrease *vs.* analyte concentration. The experimental points were fitted to the four-parameter logistic equation described above (equation 3). The mean standard curve was obtained by averaging two individual ones, previously normalized by expressing the phase decrease provided by each standard concentration as the percentage of the maximum response (maximum **s**ignal,S_{max}= 100%) in the absence of analyte.

2.7. Immunoassay protocol.

The assay procedure was as follows:

(1) Baseline stabilization: 5 min flow of working buffer (PBST).

(2) Sample injection (650 µL of standard-MAb mixture) followed by 18 min flow of working buffer.

(3) Regeneration (6 min) with 0.05 M HCl followed by working buffer (6 min).

At steps (1) and (2) the flow rate was of 20 µL min^{-1}. For step (3) it was raised to 250 µL min^{-1}. A complete assay cycle, including regeneration, takes around 35 min. Once the last assay had finished, every day crystals were washed with double distilled water, air-dried and stored at 4ºC. Each crystal could be reused for around 35 times without significant loss of basal signal.

2.8. Analytical characterization of the standard curves.

Competitive standard curves were obtained by plotting the immunoassay signal (absorbance for ELISA, phase shift for the immunosensor) against the logarithm of the analyte (38 kDa biomarker) concentration. Experimental data were

mathematically fitted to a four-parameter logistic equation (equation 3):

$$y = (A - D)/[1 + (x/C)^B] + D \qquad \text{(Eq. 3)}$$

Where:

y: Immunoassay or immunosensor signal produced by a given analyte concentration (***x***).
A: Asymptotic maximum (maximum signal, obtained in the absence of analyte).
B: Curve slope at the inflection point.
C: Analyte concentration at the inflection point, which in turn produces a 50% inhibition of the maximum signal (IC_{50} value).
D: Asymptotic minimum (background signal, corresponding to an infinite analyte concentration).

The C parameter or IC_{50} value is generally assumed as an inverse estimate of the antibody affinity to the analyte and of the immunoassay or immunosensor sensitivity. Therefore, lower IC_{50} values mean higher antibody affinity and increased assay sensitivity, and *vice versa.*

The assay limit of detection (LOD) and working range (WR) were also calculated from the parametric fitting of the standard curve. LOD was defined as the analyte concentration providing a 10% inhibition of the maximum signal (IC_{90} value). WR was defined by the analyte concentrations that produced inhibitions between 20% and 80% of the maximum signal (IC_{80}-IC_{20} range).

3. RESULTS AND DISCUSSION

3.1. Monoclonal antibody production.

The application of hybridoma technology resulted in the production of 12 cell lines secreting MAbs that recognized the recombinant 38 kDa protein from *Mycobacterium tuberculosis*. All hybridomas were cloned and stabilized, and the affinity of their corresponding antibodies was estimated by non-competitive ELISA. To this purpose, microplate wells were coated with 0.05 μg mL^{-1} of the antigen and subsequently exposed to variable antibody concentrations. **Myc-31** Mab provided the highest and more stable response against the target biomarker. Therefore, it was selected as the highest-affinity anti-38 kDa monoclonal antibody and used in further immunoassay development.

3.2. Development of a competitive ELISA for 38 kDa biomarker determination.

Checkerboard titration experiments were first conducted to find out the optimal concentrations of the antigen-antibody pair for the competitive ELISA. High enough assay signals together with competitive conditions were provided by 0.05 μg mL^{-1} of the 38 kDa antigen for coating and 0.05 μg mL^{-1} of Myc-31 MAb for the competition step. These low immunoreagent concentrations allowed obtaining a sensitive ELISA calibration curve for the target biomarker (Fig. 2).

The ELISA standard curve was mathematically fitted according to equation 3 to establish its main analytical parameters. The calculated IC_{50} value was 110 ng mL^{-1}, the LOD was 14 ng mL^{-1} of the 38 kDa protein, and the WR was estimated as 30-390 ng mL^{-1}. These low figures proved the high ELISA sensitivity, which made it a very useful analytical tool as a previous quantitative assay for 38 kDa determination and as a reference assay for the future biosensor.

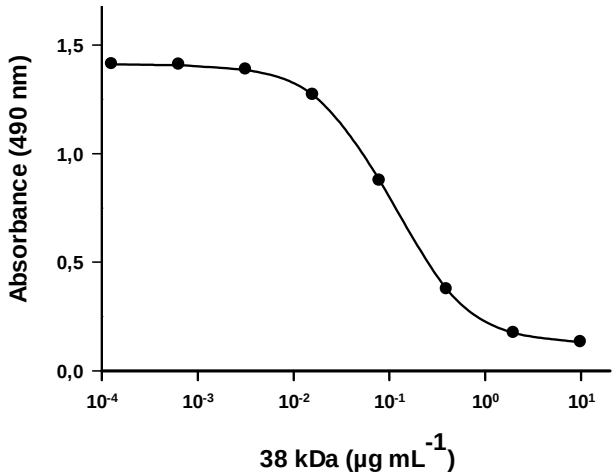

Figure 2. Calibration curve of the competitive ELISA for the 38 kDa biomarker.

3.3. Optimization of the HFF-QCM immunoassay for 38 kDa: Selection of immunoreagent concentrations.

As reported, immunosensors based on competitive immunoassays in the antigen-coated format, where the antigen is covalently immobilized to the transducer via SAM or mSAM, provide the highest QCM sensor sensitivity, regeneration capability and reproducibility [20],[30]. As for most immunoassays, operating with HFF-QCM systems requires the previous assessment of the optimal concentrations of immunoreagents involved on the antigen-antibody interaction.

Same as for ELISA, the pair (38 kDa antigen) - (Myc-31 MAb) was selected as the most suitable antigen-antibody combination to develop the HFF-QCM immunosensor. Next, several Myc-31 MAb concentrations ranging from 0.5 to 50.0 μg mL^{-1} were assayed in sensors with 50 μg mL^{-1} of immobilized 38 kDa antigen. Once delivered to the flow cell, changes on phase response were measured ($\Delta u\varphi$) as the antigen-antibody interaction took place. Results are displayed in Fig. 3.

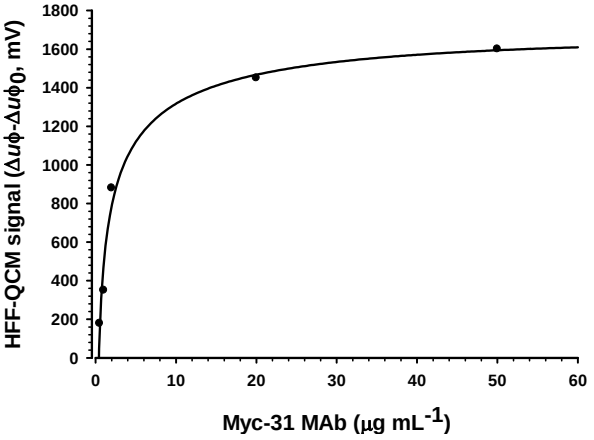

Figure 3. Signal variation obtained with a 100 MHz QCM sensor, as a function of Myc-31 MAb concentration. The sensor was functionalized with 50 μg mL^{-1} of the 38 kDa antigen.

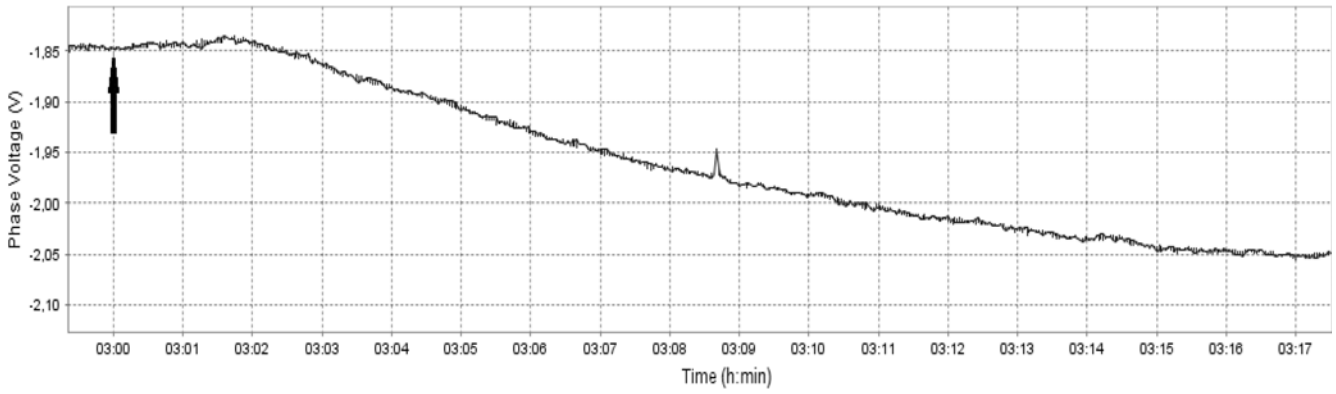

Figure 4. HFF-QCM immunosensor phase response record of an antigen-free sample. The arrow indicates the injection of Myc-31 MAb.

As expected, higher binding corresponded to increasing Myc-31 concentration. For this MAb, saturation was reached above 20 μg mL^{-1}, nearly the same antibody concentration as for the only previously described HFF-QCM immunosensor [20]. For optimal competitive assay conditions, the selected MAb concentration should provide signals below 50% of the maximum (saturation) one. In this case, the Myc-31 MAb concentration that fulfills the requirements for competitive immunoassays should be below 2 μg mL^{-1}. More precisely, the MAb concentrations which provided suitable assay signals (phase decreases corresponding to 100-300 mV) were those comprised between 0.5 and 1.0 μg mL^{-1}.

In order to refine the optimization process, 10, 20 and 50 μg mL^{-1} of the recombinant 38 kDa protein were immobilized onto 100 MHz QCM crystals and assayed in combination with Myc-31 MAb at concentrations comprised in the 0.5- 1.0 μg mL^{-1} range. From these experiments (data not shown), 20 μg mL^{-1} of 38 kDa antigen was selected as the optimal concentration for crystal functionalization, and 0,75 μg mL^{-1} of Myc-31 was chosen as the optimal MAb concentration to ensure competitive conditions and to provide optimal assay signals with minimum immunoreagent consumption.

3.4. HFF-QCM standard curves for 38 kDa biomarker: Assay sensitivity.

Fig. 4 depicts a representative real-screen record of the signal obtained when an antigen-free sample was subjected to a FHH-QCM immunosensor assay. Only Myc-31 MAb at the previously selected concentration (0.75 μg mL^{-1}) was present in the sample. The illustration shows the phase shift produced when the sensing event (binding of the antibody to the immobilized antigen) occurred. The interaction took approximately 18 min and the signal decrease was around 200 mV, high enough for competitive immunoassays purposes.

As the HFF-QCM immunosensor was working in the microgravimetric mode [20], measuring phase changes was indeed an adequate strategy to quantify the antibody-antigen interactions. Therefore, phase shifts were used to generate 38kDa antigen standard curves in the immunosensor by assaying standard samples with different concentrations of the antigen in the 10^{-3}-10^{2} μg ml^{-1} range. Regeneration of the immnuosensor between assays was achieved by treatment with 0.05 M HCl. A complete assay cycle, including regeneration, took around 35 min.

A representative mean HFF-QCM immunosensor standard curve for the 38 kDa antigen is shown in Fig. 5. It was obtained by averaging two individual curves with at least three assays for each biomarker concentration. Voltage phase shifts (**$\Delta u\varphi$**) were normalized by expressing them as:

$$100 \times \Delta u\varphi / \Delta u\varphi_0,$$

where **$\Delta u\varphi_0$** is the voltage phase decrease at zero analyte concentration (maximum signal). As for the previous ELISA, experimental points were fitted to the mathematical logistic function according to equation 3.

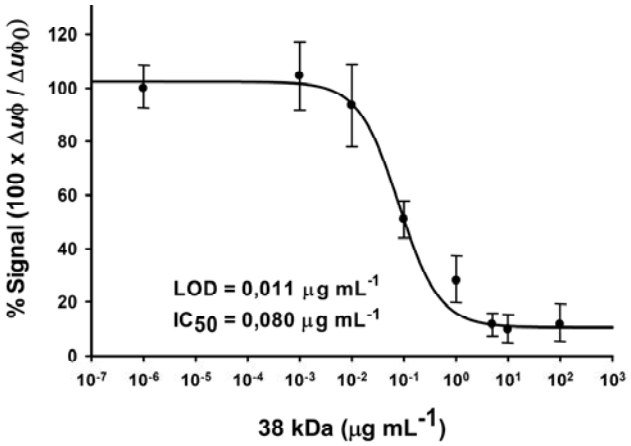

Figure 5. Calibration curve of the HFF-QCM immunosensor for the 38 kDa biomarker.

As depicted in Fig. 5 and expected for a competitive immunoassay, the 38 kDa standard curve obtained with the HFF-QCM immunosensor showed the typical sigmoidal shape associated to inhibition assays, where signal decreases as analyte concentration increases. The mathematical curve fitting parameters are shown in Table 1:

Table 1: Mathematical fitting of the HFF-QCM immunosensor standard curve for the 38 kDa antigen.

Parameter	Mean value	Std. Deviation	CV (%)
A	103.559	10.746	10.4
B	0.913	0.089	9.7
C	0.080	0.012	15.0
D	12.397	2,231	18.0

The parameter variability found was in the usual range for competitive immunoassays. Under the described optimized conditions, the sensitivity parameter ($C = IC_{50}$ value) was estimated as 80 ng mL^{-1}. The LOD and WR were 11 ng mL^{-1} and 20 – 450 ng mL^{-1} of the 38 kDa biomarker, respectively. These values were similar but even lower than those of the previously developed ELISA, which indicates that the immunosensor achieved a similar but even higher assay sensitivity and detectability than those of ELISA. In terms of molar units, the limit of detection of the HFF-QCM immunosensor was 290 pM and its working range extended from 530 pM to 12 nM of the 38 kDa antigen.

The achieved LOD clearly improves those previously reported for tuberculosis QCM immunosensors (up to 50 nM) [22],[23]. To our knowledge, only a Surface Plasmon Resonance (SPR) immunosensor was reported to be more sensitive, with a LOD of 0.1 ng mL^{-1} [11]. Moreover, the analytical parameters of the HFF-QCM immunosensor are in the range of the antigens found in biological fluids from patients suffering tuberculosis [27],[28]. Therefore, this method could presumably allow the direct analysis of the biomarker in suitable patients' samples.

CONCLUSION

On the basis of the thorough application of the most advanced immunochemical technologies (MAb production, ELISA and biosensor development), a high performance HFF-QCM immunosensor was developed for the detection of the 38 kDa tuberculosis biomarker.

High and stable assay signals were obtained using very low protein concentrations for crystal functionalization and for the integrated competitive immunoassay. This allowed to get a highly sensitive immnunosensor with IC_{50} and LOD values even lower than those of the ELISA developed with the same immunoreagents. The high detectability attained, in the picomolar range, makes this immunosensor a very promising tool for the easy, direct and sensitive detection of the tuberculosis biomarker in biological fluids such as sputum.

Current work is devoted to the validation of the HFF-QCM immunosensor. It includes and will include the native antigen purification from *Mycobacterium tuberculosis* cultures and the subsequent preparation of spiked samples, the collection of real sputum samples from tuberculosis patients, the determination of the analytical performance of the immunosensor in both types of samples (spiked and real), and finally the assessment of its biomedical significance as a diagnosis tool.

CONFLICT OF INTEREST

This study was supported by COLCIENCIAS (Colombia), Project no. 13335212865) and by AWSensors (Valencia, Spain). All of the authors: A. Montoya, C. March, Y.J. Montagut, M.J. Moreno, J.J. Manclús, A. Arnau, Y. Jiménez, M. Jaramillo, P.A. Marín and R.A. Torres declare that they have no conflict of interest.

ACKNOWLEDGEMENTS

Authors wish to express their gratitude to the following institutions: Universitat Politècnica de València (UPV, Valencia, Spain), Escuela de Ingeniería de Antioquia (EIA) – Universidad CES (Medellín, Colombia), AWSensors (Valencia, Spain).

REFERENCES

[1] World Health Organization. *World Health Statistics 2013.*WHO Press: Geneva, **2013.**

[2] Lawn, S.D.; Zumla, A.I. Tuberculosis. *Lancet*, **2011**, *6736*(10), 1–16.

[3] Keeler, E.; Perkins, M.D.; Small, P.; Hanson, C.; Reed, S.; Cunningham, J.; Aledort, J.E.; Hillborne, L.; Rafael, M.; Girosi, F.; Dye, C. Reducing the global burden of tuberculosis: the contribution of improved diagnostics. *Nature*, **2006**, *444* (Suppl. 1), 49–57.

[4] Ren, J.; He, F.; Yi, S.; Cui, X. A new MSPQC for rapid growth and detection of Mycobacterium tuberculosis. *Biosens. Bioelectron.*, **2008**, *24*(3), 403–409.

[5] McNerney, R.; Wondafrash, B. A.; Amena, K.; Tesfaye, A.; McCash, E.M.; Murray N.J. Field test of a novel detection device for Mycobacterium tuberculosis antigen in cough. *BMC Infect. Dis.*, **2010**, *10:*161.

[6] Chun, A.L. Nanoparticles offer hope for TB detection. *Nat. Nanotechnol.*, **2009**, *4*, 698–699.

[7] Lee, H.; Sun, E.; Ham, D.; Weissleder, R. Chip-NMR biosensor for detection and molecular analysis of cells. *Nat. Med.* **2008**, *14*, 869–874.

[8] Zhou, L.; He, X.; He, D.; Wang, K.; Qin, D. Biosensing technologies for Mycobacterium tuberculosis detection: status and new developments. *Clin. Dev. Immunol.*, **2011**, *2011*, 1–8.

[9] Wang, S.; Inci, F.; De Libero, G.; Singhal, A.; Demirci, U. Point-of-care assays for tuberculosis: Role of nanotechnology-microfluidics. *Biotechnol. Adv.,* **2013**, *31*, 438–449.

[10] Thiruppathiraja, C.; Kamatchiammal, P.; Adaikkappan, S.; Santhosh, D.J.; Alagar, M. Specific detection of Mycobacterium sp genomic DNA using dual labeled gold nanoparticle based electrochemical biosensor. *Anal. Biochem.*, **2011**, *417*, 73–79.

[11] Srivastava, S.K.; van Rijn, C.J.M.; Jongsma, A.A. Biosensor-based detection of tuberculosis. *RSC Adv.*, **2016**, *6*, 17559-17771.

[12] Montoya, A.; Ocampo, A., March, C. Fundamentals of Piezoelectric Immunosensors. In: *Piezoelectric Transducers and Applications*, Antonio Arnau Vives, Ed. Springer Berlin Heidelberg: Berlin, **2008**; pp. 289-306.

[13] Sauerbrey, G. Verwendung Von Schwingquarzen Zur Wägung Dünner Schichten Und Zur Mikrowägung. *Zeitschrift Fuer Phys.*, **1959**, *155*, 206–222.

[14] Montagut, Y.; García, J.V.; Jiménez, Y.; March, C.; Montoya, A.; Arnau, A. Frequency-Shift vs Phase-Shift Characterization of in-liquid Quartz Crystal Microbalance Applications. *Rev. Sci. Instrum.*, **2011**, *82*(6) 064702, 1–14.

[15] Skládal, P.; Dos Santos Riccardi, C.; Yamanaka, H.; Da Costa, P. I. Piezoelectric biosensors for real-time monitoring of hybridization and detection of hepatitis C virus. *J. Virol. Methods*, **2004**, *117*(2), 145–151.

[16] Zhou, X.; Liu, L.; Hu, M.; Wang, L.; Hu, J. Detection of hepatitis B virus by piezoelectric biosensor. *J. Pharm. Biomed. Anal.*, **2012**, *27(*1), 341–345.

[17] Minunni, M.; Tombelli, S.; Scielzi, R.; Mannelli, I.; Mascini, M.; Gaudiano, C. Detection of β-thalassemia by a DNA piezoelectric biosensor coupled with polymerase chain reaction. *Anal. Chim. Acta*, **2003**, *481*(1), 55–64.

[18] Potipitak, T. N. Diagnosis and genotyping of Plasmodium falciparum by a DNA biosensor based on quartz crystal microbalance (QCM). *Clin. Chem. Lab. Med.*, **2011**, *49*(8), 1367–1373.

[19] Dell'Atti, D.; Zavaglia, M.; Tombelli, S.; Bertacca, G.; Cavazzana, A.O.; Bevilacqua, G.; Minunni, M.; Mascini, M. Development of combined DNA-based piezoelectric biosensors for the simultaneous detection and genotyping of high risk Human Papilloma Virus strains. *Clin. Chim. Acta*, **2007**, *383*(1–2), 140–146.

[20] March, C.; García, J. V.; Sánchez, A.; Arnau, A.; Jiménez, Y.; García, P.; Manclús, J.J.; Montoya, A. High-frequency phase shift measurement greatly enhances the sensitivity of QCM immunosensors. *Biosens. Bioelectron.*, **2015**, *65*, 1–8.

[21] Parida, S. K.; Kaufmann, S.H.E. The quest for biomarkers in tuberculosis.," *Drug Discov. Today*, **2010**, *15*(3–4), 148–157.

[22] He F.; Zhang, L. Rapid diagnosis of M. tuberculosis using a piezoelectric immunosensor. *Anal. Sci.*, **2002**, *18*(4), 397–401.

[23] Hiatt L.A.; Cliffel, D.E. Real-time recognition of Mycobacterium tuberculosis and lipoarabinomannan using the quartz crystal microbalance. *Sens. Actuator B-Chem.*, **2012**, *174*, 245–252.

[24] McNerney, R.; Maeurer, M.; Abubakar, I.; Marais, B.; Mchugh, T.D.; Ford, N.; Weyer, K.; Lawn, S.; Grobusch, M. P.; Memish, Z.; Squire, S. B.; Pantaleo, G.; Chakaya, J.; Casenghi, M.; Migliori, G.B.; Mwaba, P.; Zijenah, L.; Hoelscher, M.; Cox, H.; Swaminathan, S.; Kim, P.S.; Schito, M.; Harari, A.; Bates, M.; Schwank, S.; O'Grady, J.; Pletschette, M.; Ditui, L.; Atun, R.; Zumla, A.; "Tuberculosis Diagnostics and Biomarkers: Needs, Challenges, Recent Advances, and Opportunities. *J. Infect. Dis.*, **2012**, *205* (Suppl. 2), 47–58.

[25] Walzl, G.; Ronacher, K.; Djoba Siawaya, J.F.; Dockrell, H.M. Biomarkers for TB treatment response: challenges and future strategies. *J. Infect.*, **2008**, *57*(2), 103–109.

[26] Devi, K.R.U.; Kumar, K.S.S.; Ramalingam, B.; Alamelu, R.; Purification and characterization of three immunodominant proteins (38, 30, and 16 kDa) of Mycobacterium tuberculosis. *Protein Expr. Purif.*, **2002**, *24*(2), 188–95.

[27] Attallah, A.M.; Abdel Malak, C.A.; Ismail, H.; El-Saggan, A.H.; Omran, M.M.; Tabll, A.A. Rapid and simple detection of a Mycobacterium tuberculosis circulating antigen in serum using dot-ELISA for field diagnosis of pulmonary tuberculosis. *J. Immunoassay Immunochem.*, **2003**, *24*(1), 73–87.

[28] Steingart, K.R.; Dendukuri, N.; Henry, M.; Schiller, I.; Nahid, P.; Hopewell, P.C.; Ramsay, A.; Pai, M.; Laal, S. Performance of purified antigens for serodiagnosis of pulmonary tuberculosis: a meta-analysis. *Clin. Vaccine Immunol.*, **2009**, *16*(2), 260–76.

[29] Nowinski, R.C.; Lostrom, M.E.; Tam, M.R.; Stone, M.R.; Burnette, W.N. The Isolation of Hybrid Cell Lynes Producing Monoclonal Antibodies Against the p15(E) Protein of Ecotropic Murine Leukemia Viruses. *Virology*, **1979**, *93*, 111–12.

[30] March, C.; Manclús, J.J.; Jiménez, Y.; Arnau, A.; Montoya, A. A piezoelectric immunosensor for the determination of pesticide residues and metabolites in fruit juices. *Talanta*, 2009, 78(3), 827–833.

Accepted: June 19, 2016